Chemical ionization mass spectrometry technique for detection of dimethylsulfoxide and ammonia

J. B. Nowak,[1] L. G. Huey, and F. L. Eisele[2]
School of Earth and Atmospheric Sciences, Georgia Institute of Technology, Atlanta, Georgia, USA

D. J. Tanner,[3] R. L. Mauldin III, C. Cantrell, and E. Kosciuch
Atmospheric Chemistry Division, National Center for Atmospheric Research, Boulder, Colorado, USA

D. D. Davis
School of Earth and Atmospheric Sciences, Georgia Institute of Technology, Atlanta, Georgia, USA

Received 12 July 2001; revised 10 December 2001; accepted 21 December 2001; published 28 September 2002.

[1] A chemical ionization mass spectrometer (CIMS) was used to study reactions of protonated ethanol clusters $(C_2H_5OH)_nH^+$ with dimethylsulfoxide (DMSO), dimethylsulfone ($DMSO_2$), ammonia (NH_3), and a series of nonmethane hydrocarbons (NMHCs) and volatile organic compounds (VOCs). The reactivity of the $(C_2H_5OH)_nH^+$ cluster ions is a function of cluster size with reactivity decreasing as cluster size increases. Ethanol cluster ion distributions that formed at atmospheric pressure from 24 ppbv, 900 ppmv, and 1% ethanol/N_2 gas mixtures were studied. Small $(C_2H_5OH)_nH^+$ clusters, those formed using the 24 ppbv ethanol/N_2 mixture, react at or near the collisional rate with DMSO, NH_3, acetone, and methyl vinyl ketone (MVK). The effective ion molecule rate coefficients are 1.8×10^{-9}, 1.5×10^{-9}, 1.0×10^{-9}, and 1.6×10^{-9} cm^3 molecule^{-1} s^{-1}, respectively. Only DMSO and NH_3 react efficiently with the two larger $(C_2H_5OH)_nH^+$ cluster ion distributions studied. The effective rate coefficients for DMSO and NH_3 with the 900 ppmv ethanol cluster ion distribution are 1.5×10^{-9} and 0.7×10^{-9} cm^3 molecule^{-1} s^{-1}, respectively. The effective rate coefficient for DMSO with the 1% ethanol/N_2 mixture is 0.35×10^{-9} cm^3 molecule^{-1} s^{-1}, while NH_3 reaches equilibrium with this cluster ion distribution. Experiments show that large $(C_2H_5OH)_nH^+$ ion clusters must be used at relative humidities greater than 50% at 20°C to prevent formation of and subsequent interferences from H_3O^+ ions. These results demonstrate that the $(C_2H_5OH)_nH^+$ ion chemistry can selectively detect DMSO and NH_3 under most ambient atmospheric conditions with high sensitivity. *INDEX TERMS:* 0305 Atmospheric Composition and Structure: Aerosols and particles (0345, 4801); 0365 Atmospheric Composition and Structure: Troposphere—composition and chemistry; 0394 Atmospheric Composition and Structure: Instruments and techniques; *KEYWORDS:* chemical ionization mass spectrometry, CIMS, dimethylsulfide, DMSO, ammonia, ethanol ion chemistry

Citation: Nowak, J. B., L. G. Huey, F. L. Eisele, D. J. Tanner, R. L. Mauldin III, C. Cantrell, E. Kosciuch, and D. D. Davis, Chemical ionization mass spectrometry technique for the detection of dimethylsulfoxide and ammonia, *J. Geophys. Res.*, *107*(D18), 4363, doi:10.1029/2001JD001058, 2002.

1. Introduction

[2] Chemical Ionization Mass Spectrometry (CIMS) has been used to selectively measure many atmospheric trace gases with high sensitivity. The list of species includes: the hydroxyl radical (OH), sulfuric acid (H_2SO_4), methane sulfonic acid (MSA), and nitric acid (HNO_3) [*Eisele and Tanner*, 1991; *Huey et al.*, 1998; *Mauldin et al.*, 1998; *Viggiano*, 1993]. One important feature of the CIMS method is its ability to perform measurements on fast timescales (i.e., 1 s). For many trace gases, fast time resolution measurements are essential for testing our understanding of sources and sinks. One such species falling into the above category is dimethylsulfoxide (DMSO).

[3] DMSO is believed to be one of the major products of the OH-initiated oxidation of dimethylsulfide (DMS)

[1]Now at Aeronomy Laboratory, NOAA, Boulder, Colorado, USA.
[2]Also at Atmospheric Chemistry Division, National Center for Atmospheric Research, Boulder, Colorado, USA.
[3]Now at School of Earth and Atmospheric Sciences, Georgia Institute of Technology, Atlanta, Georgia, USA.

0148-0227/02/2001JD001058

[*Arsene et al.*, 1999; *Davis et al.*, 1998; *Sorensen et al.*, 1996; *Turnipseed et al.*, 1996].

$$OH + DMS \rightarrow\rightarrow\rightarrow SO_2, MSA, DMSO, DMSO_2, \text{other products.} \quad (1)$$

DMS is a byproduct of marine phytoplankton metabolic activity, and its release from the ocean surface accounts for the largest fraction of biogenic gas-phase sulfur emissions [*Bates et al.*, 1992; *Berresheim et al.*, 1995]. It has been hypothesized that the formation of sulfate aerosols from DMS oxidation products may significantly influence the Earth's radiation budget and possibly regulate climate [*Charlson et al.*, 1987]. DMS oxidation occurs by a complex mechanism with multiple steps that are currently the focus of many laboratory and field investigations [*Barone et al.*, 1996; *Chen et al.*, 2000; *Hynes et al.*, 1995; *Turnipseed et al.*, 1996; *Yin et al.*, 1990a, 1990b]. Critical to assessing the affect of DMS oxidation on climate is understanding the chemical and physical processes that control the fate of these products in the atmosphere.

[4] In the atmosphere DMSO reacts rapidly with OH

$$DMSO + OH \rightarrow\rightarrow \text{products.} \quad (2)$$

There is, however, considerable debate as to the products of reaction (2) under atmospheric conditions. *Barnes et al.* [1989] and *Sorensen et al.* [1996] suggest that reaction (2) produces SO_2 and $DMSO_2$, though they disagree as to the yield of each product, while *Urbanski et al.* [1998] suggests that methane sulfinic acid (MSIA) is a significant product. All the studies agree that reaction (2) leads to a DMSO photochemical lifetime of less than 1 hour for typical midday marine boundary layer OH levels. Another loss process for atmospheric DMSO is scavenging by cloud droplets or sea salt aerosol [*Davis et al.*, 1998; *De Bruyn et al.*, 1995]. Therefore, depending on aerosol loading, the overall lifetime of DMSO in the marine boundary layer can be even shorter than that due to photochemistry alone. The short photochemical lifetime highlights the need for fast time resolution measurements of DMSO in order to gain a comprehensive understanding of DMS oxidation.

[5] There are few measurements of gas-phase DMSO reported in the literature. The techniques utilized include: gas chromatography, gas chromatography/mass spectrometry, and a Cofer mist chamber [*Bandy et al.*, 1996; *Harvey and Lang*, 1986; *Sciare and Mihalopoulos*, 2000]. One common characteristic of all of these methods is a sampling resolution of 30 min or longer. Under these conditions a detailed study of DMS oxidation becomes quite difficult.

[6] *Berresheim et al.* [1993] developed a CIMS method to measure DMSO on a subminute timescale using NH_4^+ core reagent ions. NH_3 has a proton affinity (PA) (204 kcal/mol) higher than water (166 kcal/mol) and lower than DMSO (211 kcal/mol) [*Hunter and Lias*, 2000]. Therefore, NH_4^+ ions proton transfer with DMSO in ambient air to form $DMSOH^+$. The estimated limit of detection for a 60-s integration period has been reported at 0.5 pptv. A limitation of this ion chemistry, however, is the inability to measure other atmospheric trace gases with PA equal to or less than 204 kcal/mol. One such trace gas is NH_3.

[7] NH_3 is another important atmospheric trace gas for which there are few fast time response methods available. The measurement techniques include: photofragmentation/laser-induced fluorescence, denuder sampling/chemiluminescence detection, denuder sampling/ion chromatography, and filter pack sampling/colorimetric analysis [*Williams et al.*, 1992]. Recent laboratory and field measurements have led to the hypothesis that ammonia is potentially important in moderating particle nucleation and growth [*Coffman and Hegg*, 1995; *Weber et al.*, 1998]. The primary goal of this work has been to find an appropriate reagent ion for detecting both DMSO and NH_3 using the same technique. The possibility explored here is protonated ethanol, $(C_2H_5OH)H^+$.

[8] Ethanol has a proton affinity (185.6 kcal/mol) higher than water and lower than both DMSO and NH_3 [*Hunter and Lias*, 2000]. However, $(C_2H_5OH)H^+$ efficiently clusters with any available ethanol to form an equilibrium distribution of protonated ethanol cluster ions, $(C_2H_5OH)_nH^+$, where the range of n depends on temperature and the concentration of C_2H_5OH. However, the reactivity of $(C_2H_5OH)_nH^+$ is quite different from that of $(C_2H_5OH)H^+$, for example, dependent on *n*, the cluster size [*Feng and Lifshitz*, 1995].

[9] As a starting point in developing a CIMS method for detecting both DMSO and NH_3, the effective rate coefficients for reactions of $(C_2H_5OH)_nH^+$ with DMSO, NH_3, $DMSO_2$, DMS, a series of nonmethane hydrocarbons (NMHCs), and a series of volatile organic compounds (VOCs) were measured (see Tables 1 and 2). The sensitivity of this ion chemistry for the detection of DMSO and NH_3 and the possibility of artifact DMSO production from ambient DMS oxidation within the instrument were also examined. Finally, a new ion-molecule reactor, specifically designed for aircraft applications, was characterized and then used to measure DMSO in ambient air on the NASA P-3B as part of the PEM-Tropics B field program.

2. Experiment

2.1. Gas Standards

[10] Isotopically labeled C^{13} DMSO and C^{13} $DMSO_2$ permeation devices were manufactured by VICI Metronics, Inc. using 99% pure isotopically labeled compounds from Icon Services. These devices were maintained at a constant temperature and pressure. The concentrations of DMSO and $DMSO_2$ were controlled with a dynamic dilution system similar to that described by *Goldan et al.* [1986]. The permeation rates of each device were determined gravimetrically by the manufacturer and are traceable to NIST standards. The combined uncertainty of the C^{13} DMSO permeation tube and dilution system is estimated at ±50% and primarily reflects the uncertainty associated with the emission rate of the permeation tubes. The combined uncertainty of the C^{13} $DMSO_2$ permeation tube and dilution is estimated at ± a factor of 5 and reflects additional difficulties associated with that particular permeation device.

[11] NH_3 concentrations were determined by monitoring the absorption of the 185-nm mercury atomic line. An NH_3 absorption cross section at 185 nm of 4.3×10^{-18} cm^2 $molecule^{-1}$ was used [*Lovejoy*, 1999]. The nonmethane hydrocarbons (NMHCs) and volatile organic compounds

Table 1. Species Found to React With $(C_2H_5OH)_nH^+$ With Ion Molecule Rate Coefficients $>2 \times 10^{-12}$ cm^3 $molecule^{-1}$ s^{-1}[a]

Species	P.A.	k_{Cal}	k_{Low}	k_{mid}	k_{High}
DMSO	211.4	2.2	1.8	1.5	0.35
NH_3	204	1.9	1.5	0.7	>0.0025[b]
Acetone	194	1.9	1.0	nr	nr
MVK	199.5	–	1.6	nr	nr
$DMSO_2$	?	–	0.1–1.0	nr	nr

[a] P.A., proton affinity (kcal/mol) [*Hunter and Lias*, 2000]; k_{Cal}, calculated collisional rate constant (10^{-9} cm^3 $molecule^{-1}$ s^{-1}) [*Su and Chesnavich*, 1982]; k_{Low}, 24 ppbv ethanol/N_2 reagent mixture (10^{-9} cm^3 $molecule^{-1}$ s^{-1}); k_{Mid}, 900 ppmv ethanol/N_2 reagent mixture (10^{-9} cm^3 $molecule^{-1}$ s^{-1}); k_{High}, 1% ethanol/N_2 reagent mixture (10^{-9} cm^3 $molecule^{-1}$ s^{-1}); nr, rate constant $< 2 \times 10^{-12}$ cm^3 $molecule^{-1}$ s^{-1}.
[b] System equilibrates.

(VOCs) used in these experiments were obtained from Scott Gases and Apel-Riemer Environmental, Inc. The mixing ratios of the NMHC and VOC standards were between 10 and 20 ppmv.

2.2. Ion-Molecule Reactor

[12] The CIMS apparatus consists of two sections, an ion-molecule reactor where the sampling and chemical ionization is performed and a vacuum system housing a quadrupole mass spectrometer and an electron multiplier detector. Two mass spectrometers were used in this work. The laboratory experiments were performed on the Georgia Tech dual channel diffusion pump system previously described by *Eisele and Tanner* [1993]. The ambient air measurements were performed on the top channel of the four-channel NCAR CIMS system as described by *Mauldin et al.* [2001]. In both cases the same ion-molecule reactor was used.

[13] The ion-molecule reactor consists of two sections, the transverse ion source and the transport tube, as shown in Figure 1. The transverse ion source is similar to that described by *Eisele and Hanson* [2000]. The ion source is a $7 \times 8 \times 2.5$ cm teflon block with a 1.9-cm-diameter hole machined through the center. A 9-cm-long by 1.9-cm-inner-diameter teflon tube fits snugly into the teflon block mating with the center hole to form the sampling inlet. Ambient air or dry N_2 is sampled through the inlet at 4 SLPM. A radioactive ion source, ^{241}Am, and the transport tube are located on opposite sides of the sampling tube. Between the radioactive source and transport tube is the ion-molecule reaction region (see Figure 1). The stainless steel transport tube is 22.86 cm long with a diameter of 0.762 cm and a 0.025-cm-diameter orifice located at its top. A buffer gas of dry N_2 is continuously flowed in front of the orifice to minimize any ambient air or un-ionized reagent gas from entering the transport tube.

[14] The two advantages of using this type of ion-molecule reactor on an aircraft platform are that (1) the transport tube provides a convenient way to extend the sampling inlet outside of an airplane's boundary layer, and 2) contact between the inlet wall and the ambient air sample is minimized by aligning the sampling tube with the ambient air flow, thus allowing for a straight sampling path into the reaction region. Minimal wall interactions should also increase instrument response time by inhibiting reversible desorption from the walls.

2.3. Reaction Time

[15] The protonated ethanol cluster ions are produced by flowing 1 SLPM of an ethanol/N_2 mixture over a foil containing ^{241}Am that releases α particles, which form $(C_2H_5OH)H^+$ through a series of reactions. These ions rapidly cluster with ethanol to form an equilibrium distribution of $(C_2H_5OH)_nH^+$. The $(C_2H_5OH)_nH^+$ ions are accelerated across the reaction region through the path of the ambient sample by an electrical field produced by applying a potential of 1.6 kV to the radioactive ion source and 100 V to the transport tube. When in the reaction region, the $(C_2H_5OH)_nH^+$ ions react with some higher proton affinity species via

$$(C_2H_5OH)_nH^+ + X \rightarrow H^+(X)(C_2H_5OH)_{n-y} + y(C_2H_5OH) \quad (3)$$

$$H^+(X)(C_2H_5OH)_{n-y} + M \rightarrow\rightarrow\rightarrow XH^+ + (n-y)C_2H_5OH + M, \quad (4)$$

where, for example, X is DMSO. Reaction (4) represents multistep ion declustering processes occurring in the collision dissociation chamber (CDC) and, as discussed later in the text, in the transport tube.

[16] The drift time (i.e., reaction time) of the ions across the reaction region can be calculated as

$$t_d = \frac{L^2}{kV}, \quad (5)$$

where L is the length of the reaction region, V is the electrical potential across the region, and k is the mobility of

Table 2. Species Found to React With $(C_2H_5OH)_nH^+$ With Ion Molecule Rate Coefficients $<2 \times 10^{-12}$ cm^3 $molecule^{-1}$ s^{-1}[a]

Species	P.A.	Species	P.A.	Species	P.A.
Methane	129.9	trans-2-butene	179	2-pentanone	199.8
Acetylene	153.3	n-butane	?	ethyl acetate	199.7
Ethylene	162.6	isobutane	162	cyclobutene	187.5
Ethane	142.5	isopropanol	189.5	α-pinene	?
Methanol	180.3	isobutylene	191.7	ethyl Acetate	?
Propyne	179	methylcyclo-hexane	?	1,3-butadiene	187.2
Propylene	179.6	methacrolein	193.3	m-xylene	194.1
DMS	198.6	Cyclopentane	?	o-xylene	190.2
Isoprene	189.5	methylcyclo-pentane	?	ethylbenzene	188.3
Toluene	187.4	4-methyl-2-pentene	?	methylbutenol	?
1-butene	?	3-methyl-2-pentene	194.3	methyl isobutyl ketone	?
cis-2-butene	?	2-methyl-2-pentene	194		

[a] P.A., proton affinity (kcal/mol) [*Hunter and Lias*, 2000].

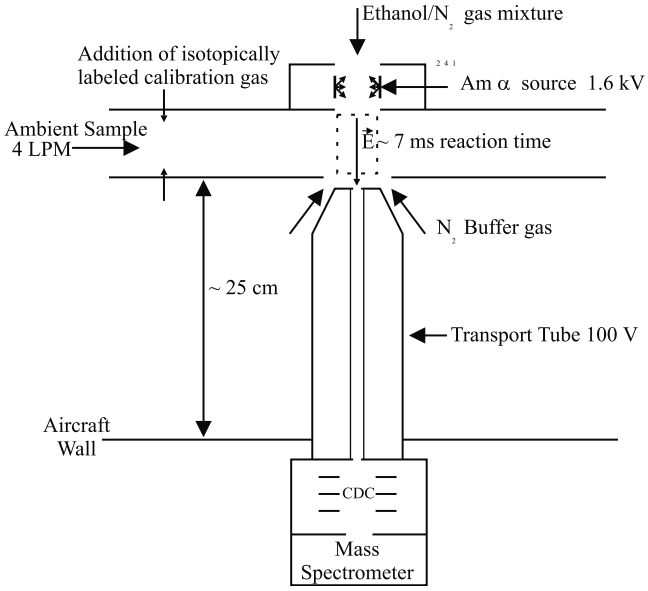

Figure 1. Diagram of the ion-molecule reactor used in this study.

the ion. However, there are two difficulties to applying equation (5) to the setup used here. First, k is unknown because the ethanol cluster size distribution in the reaction region is impossible to predict due to a lack of thermodynamic parameters. Second, this formula determines the drift time for ions between two infinitely long parallel plates and does not take into account the specific geometries of the ion-molecule reactor or any dielectric effects from the teflon housing to the electric field. Therefore, an independent determination of the reaction time was obtained using SF_6^- as the reagent ion and adding a SO_2/N_2 mixture to the ion-molecule reactor to estimate the effective electric field strength.

[17] The rate constant for the $SF_6^- + SO_2$ reaction has been well established as 1.0×10^{-9} cm^3 molecule^{-1} s^{-1}, independent of temperature, pressure, and carrier gas [*Arnold et al.*, 2000; *Ferguson*, 1976; *Huey et al.*, 1995; *Streit*, 1982]. The reaction time was calculated from measuring the decay of SF_6^- as a function of the SO_2 concentration. From these experiments a reaction time of 7 ms was obtained. Using this reaction time, the reaction region length (L = 1.9 cm), and 1.90 cm^2 V^{-1} s^{-1} as the SF_6^- ion mobility [*Lakdawala and Moruzzi*, 1980], the effective voltage (V_{eff}) is calculated to be 270 V.

[18] The largest uncertainty with estimating the reaction time lies in the calculation of the ion mobility of the ethanol cluster ion distribution. The relationship between ion mobility and mass has been difficult to quantify [e.g., *Bohringer et al.*, 1987; *Tammet*, 1995]. Along with mass, ion structure is known to affect mobility [*Kim and Spangler*, 1985]. Again, since the protonated ethanol cluster size distribution is unknown, it is even more difficult to relate mass and ion structure to mobility of the ethanol cluster ion distribution. *Makela et al.* [1996] measured the mobility of acetone cluster ions produced in a manner similar to the ethanol cluster ions in this study (i.e., flowing 1000 ppmv of acetone over a radioactive ion source) at 1.3–1.5 cm^2 V^{-1} s^{-1}. Since the mass of acetone is similar to that of ethanol (58–46 amu), it is reasonable to assume that the ion mobility of the protonated ethanol cluster ions in this study is similar. Furthermore, data from *Kilpatrick* [1971] suggests that the ion mobility only changes approximately by a factor of 2 for an order of magnitude change in mass from 47 to 461 amu. Therefore, using 1.4 cm^2 V^{-1} s^{-1}, the midpoint of the range from the acetone cluster study, as the ion mobility, the reaction time is estimated from equation (3) at 10 ms. Given the results of *Kilpatrick* [1971], this estimate is probably reasonable within a factor of 2.

2.4. Transport Tube Effects

[19] Since water from the ambient sample and ethanol from the reagent gas are prevented from entering the transport tube by the use of N_2 as a buffer gas in front of the transport tube orifice, the distribution of $(C_2H_5OH)_nH^+$ cluster ions in the transport tube is dramatically altered from that in the reaction region. Weakly bound cluster ions dissociate in the transport tube allowing the $(C_2H_5OH)_nH^+$ ions to reach a new equilibrium distribution. The minimum cluster bond strength needed to transverse the transport tube has been estimated at 20–21 kcal/mol. Thus, the transport tube greatly affects what is detected since clusters with a bond energy of less than 20–21 kcal/mol will dissociate in the transport tube before being detected. As a result, the transport tube makes the observed mass spectrum less complicated and easier to interpret.

[20] Unfortunately, due to the transport tube setup used in this work, it is impossible to know the detailed size distribution of ethanol clusters in the reaction region. However, it is known that the observed ethanol cluster distribution is quite different from that in the reaction region. Because of this, in order to qualitatively test for reactivity as a function of cluster size, experiments were performed using ethanol/N_2 reagent gas mixtures of 24 ppbv, 900 ppmv, and 1% C_2H_5OH to produce different size $(C_2H_5OH)_nH^+$ reagent ion distributions. In all cases, the dominant $(C_2H_5OH)_nH^+$ clusters observed in the mass spectra were the monomer, $(C_2H_5OH)H^+$, the dimer, $(C_2H_5OH)_2H^+$, and the trimer, $(C_2H_5OH)_3H^+$. Since the ΔH_{rxn} of

$$(C_2H_5OH)_2H^+ + C_2H_5OH \rightarrow (C_2H_5OH)_3H^+ \qquad (6)$$

has been reported as −21.4 kcal/mol [*Feng and Lifshitz*, 1995], it is not surprising that no evidence of $(C_2H_5OH)_4H^+$ or larger is seen in the mass spectra (i.e., the larger clusters dissociate in the transport tube before detection). Under the 24 ppbv ethanol conditions, the monomer and dimer were the only clusters observed. At the higher ethanol levels, the monomer and dimer signals increased and now the trimer was also observed. These results, particularly the appearance of a new cluster (i.e., the trimer), suggest that there are larger ethanol clusters in the reaction region under the higher ethanol conditions than under the 24 ppbv ethanol conditions, as expected.

3. Results

3.1. Effective Rate Coefficients

[21] Effective rate coefficients were determined for the ion molecule reaction of $(C_2H_5OH)_nH^+$ with DMSO, NH_3,

CH_4, DMS, and select NMHCs and VOCs using 24 ppbv, 900 ppmv, and 1% ethanol/N_2 reagent gas mixtures. The effective rate coefficients were determined by monitoring the depletion of the total ethanol signal (i.e., the sum of the monomer, dimer, and trimer signals) as a function of the neutral reactant added to a dry N_2 sample flow. Given the combined uncertainties in the estimated reaction time and the gas standard dilutions, the uncertainty in the effective ion-molecule rate coefficients reported here is estimated at a factor of 2.

[22] The measured effective rate coefficients for the ion molecule reactions of $(C_2H_5OH)_nH^+$ are reported in Tables 1 and 2 along with the proton affinities of the neutral reactants. Listed in Table 2 are all species tested that react with $(C_2H_5OH)_nH^+$ at $< 2 \times 10^{-12}$ cm^3 molecule^{-1} s^{-1} under all ethanol conditions. Calculated collision rate coefficients, determined by the method of *Su and Chesnavich* [1982], in the limit that the ethanol cluster size approaches infinity, are reported for selected reactions. As shown in Table 1, DMSO, NH_3, acetone, and methyl vinyl ketone (MVK) react with small protonated ethanol clusters (i.e., 24 ppbv ethanol/N_2 reagent gas mixture) at or near the calculated collision rate. The effective rate coefficients are: 1.8×10^{-9}, 1.5×10^{-9}, 1.0×10^{-9}, and 1.6×10^{-9} cm^3 molecule^{-1} s^{-1}, respectively. $DMSO_2$ was also found to react with small protonated ethanol clusters at or near the gas kinetic rate, however, the additional uncertainty in the $DMSO_2$ standard has prevented a more precise determination from being made. Only DMSO and NH_3 react efficiently with the larger ethanol cluster ion distribution (i.e., 900 ppmv ethanol/N_2 reagent gas mixture) with effective rate coefficients of 1.5×10^{-9} and 0.7×10^{-9} cm^3 molecule^{-1} s^{-1}. DMSO and NH_3 are also the only species to react efficiently with the largest ethanol cluster ion distribution (i.e., 1% ethanol/N_2 reagent gas mixture), however, the DMSO effective ion molecule rate has slowed to 0.35×10^{-9} cm^3 molec^{-1} s^{-1}, while only a lower limit on the NH_3 reaction can be given because the system equilibrates.

$$(C_2H_5OH)_nH^+ + NH_3 \Leftrightarrow (NH_3)(C_2H_5OH)_lH^+ + nC_2H_5OH. \quad (7)$$

The ratio of product ions to reactant ions,

$$\frac{(NH_3)(C_2H_5OH)_lH^+}{(C_2H_5OH)_nH^+},$$

is temperature and ethanol concentration dependent. In the laboratory at 21°C and 1% ethanol/N_2 reagent gas mixture this ratio is 2.5×10^{-12}. These experiments clearly show that the reactivity of the $(C_2H_5OH)_nH^+$ ions is a function of cluster size.

3.2. Relative Humidity Tests

[23] The $(C_2H_5OH)_nH^+$ ion distribution was studied as a function of relative humidity (RH). At low ethanol concentrations (i.e., 24 ppbv ethanol) the $(C_2H_5OH)_nH^+$ ions are converted to the water clusters $(H_2O)_2H^+$ (37 amu) and $(H_2O)_3H^+$ (55 amu) for RH > 50%. But for the same RH under the 900 ppmv and 1% ethanol conditions, the dominant peaks are the ethanol monomer, dimer, and trimer. At RH < 25% the ethanol ion peaks dominate independent of ethanol concentration. Further experiments were performed by varying the ethanol concentration in the reagent gas mixture from 400 to 2200 ppmv while keeping the UHP zero air stream at a constant 75% RH. These experiments indicate that for reagent gas mixtures with less than 900 ppmv of ethanol the $(C_2H_5OH)_nH^+$ ions are converted to water clusters. Thus, these results suggest that at high RH (i.e., >75%) it is necessary to use a reagent gas mixture greater than 900 ppmv of ethanol to preserve the $(C_2H_5OH)_nH^+$ chemistry. It is important to maintain the $(C_2H_5OH)_nH^+$ chemistry because $(H_2O)_mH^+$ is more reactive than $(C_2H_5OH)_nH^+$ and shifting the ion chemistry to $(H_2O)_mH^+$ would decrease the selectivity of this technique.

[24] Additional experiments were performed to examine the effect of H_2O on the effective ion molecule rate constants for DMSO and NH_3. This was done with a 900 ppmv ethanol/N_2 reagent gas mixture by adding a constant amount of DMSO, 70 pptv, or NH_3, 400 pptv, while varying the RH in the UHP zero air sample from 0 to 85%. Under these conditions less than 20% of the total ethanol signal was converted to water clusters, thereby preserving the $(C_2H_5OH)_nH^+$ chemistry. More importantly, the effective ion molecule rate coefficients for DMSO and NH_3 changed by less then 20% from 0 to 85% RH. Thus, these results suggest that when using reagent gas mixtures containing 900 ppmv of ethanol or greater then the sensitivity for detection of DMSO and NH_3 is not very humidity dependent.

3.3. DMS Interferences

[25] The species benzene (C_6H_6) and methanol (CH_3OH) could give ion products ($C_6H_6H^+$ or $CH_3OH-C_2H_5OHH^+$) that have the same mass as $DMSOH^+$. However, since neither C_6H_6 nor CH_3OH were observed to react with $(C_2H_5OH)_nH^+$, they are not considered to be significant interferences in the detection of DMSO. Recalling that DMSO is produced by the oxidation of DMS, a potential interference is artifact DMSO production by ion molecule processes from ambient DMS present in the reaction region. To test for this possibility, DMS was added to a UHP zero air sample flow in concentrations ranging from 600 pptv to 69 ppbv under the following conditions: low RH (25%), high RH (80%), low RH with 200 ppbv O_3, and high RH with 200 ppbv O_3. The results showed that DMS did not react with $(C_2H_5OH)_nH^+$ under any of the above conditions to produce a product at the mass of $DMSH^+$, $DMSOH^+$, or C^{13} $DMSOH^+$.

3.4. Ambient Air Tests

[26] The protonated ethanol ion chemistry was used to measure DMSO on one channel of the NCAR four-channel CIMS system deployed on the NASA P-3B aircraft during the GTE-PEM Tropics B field program in March/April of 1999. To maximize the selectivity during these measurements a 1% ethanol/N_2 reagent gas mixture was used. The sensitivity of the instrument to DMSO was measured to be ~1 count per second (Hz) per pptv of DMSO at a total ethanol signal of 10 kHz relative to the calibration C^{13} DMSO. This agrees quite well with the sensitivity of 0.9 Hz per pptv estimated from the experimentally determined

effective rate coefficient under the 1% ethanol conditions. Measurement backgrounds were performed by overfilling the inlet with N_2 or UHP zero air. The background signal at the DMSO product ion mass was found to be no greater than 1 Hz (i.e., 1 pptv) which gives a limit of detection for DMSO of 0.50 pptv for a 60-s integration period. As expected, the DMSO sensitivity was not affected by ambient relative humidity under 1% ethanol conditions to within ±20%.

[27] Figure 2 compares a mass spectrum taken in the boundary layer at 75% RH during flight 16 of PEM-Tropics B, Figure 2a, with one taken in the laboratory at 80% RH using a 1% ethanol/N_2 reagent gas mixture, Figure 2b. Note that the ion signal axis is linear from 0 to 1000 Hz and logarithmic above 1000 Hz. The discrepancy in total ion signal between the two spectra is primarily a result of the difference in pumping speeds between the field and laboratory instruments. As seen in Figure 2, the ethanol cluster peaks dominate both spectra indicating the preservation of the $(C_2H_5OH)_nH^+$ ion chemistry under these high RH conditions. Also seen in Figure 2b are NH_4^+ and $(C_2H_5OH)H^+ \cdot NH_4^+$ due to NH_3 contamination in the laboratory.

[28] Figure 3 presents a time series plot of DMSO taken during the midday boundary and buffer layer sampling runs during flight 16 of PEM-Tropics B. The data shown here were recorded at 15-s time resolution. This time series highlights the response time of the technique. Here one can easily see the sharp change in DMSO levels when switching between the boundary and buffer layers. This suggests that the response time of this technique is faster than 15 s, making it highly suitable for aircraft studies. The data also show significant levels of DMSO in both the boundary and buffer layers. As expected, boundary layer DMSO levels were 2–3 times greater than those observed in the buffer layer. A more detailed comparison of these observations with model simulations is presented by *Nowak et al.* [2001].

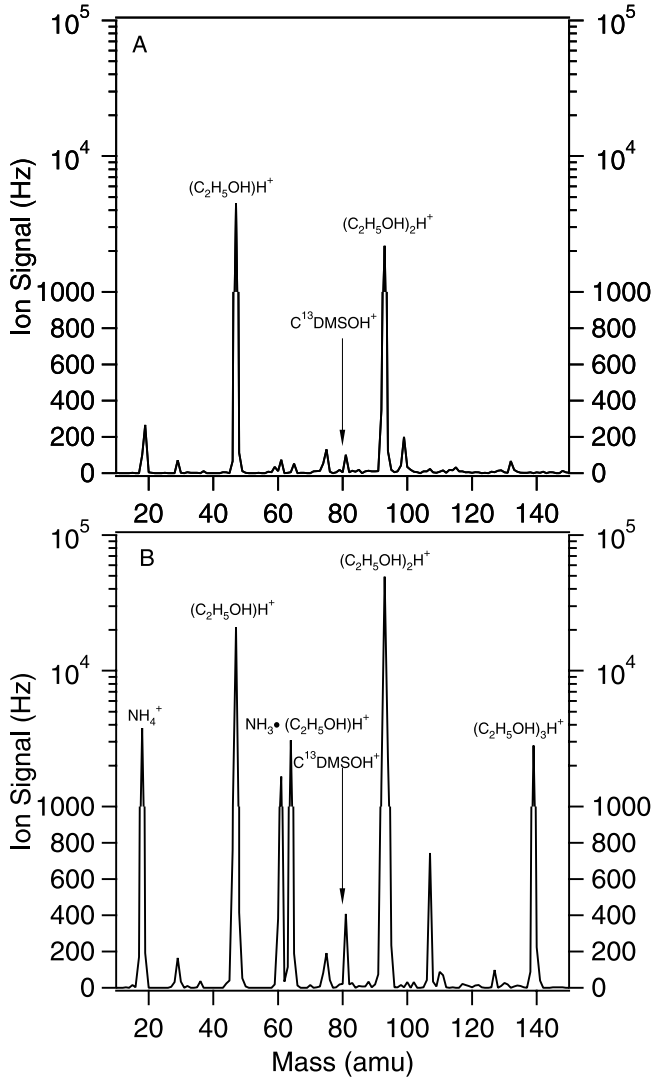

Figure 2. (a) Mass spectrum taken in the boundary layer at 75% relative humidity during PEM-Tropics B flight 16. (b) Mass spectrum taken in the laboratory at 80% relative humidity. (Note, the *y* axis is linear from 0 to 1000 Hz and logarithmic above 1000 Hz.) Dominant peaks in both spectra at high relative humidity are ethanol monomer and dimer. In Figure 2b, the peak present at 61 amu is isopropanol impurity present in the ethanol used to generate the reagent ions.

4. Summary and Discussion

[29] Overall, the protonated ethanol cluster ion chemistry presented in this work appears to be a highly selective and sensitive method for detecting certain atmospheric trace gases. However, controlling cluster size is critical for utilizing this ion chemistry in field studies. As shown in Table 2, many species with PA > C_2H_5OH do not react with any size $(C_2H_5OH)_nH^+$ clusters studied. As indicated by Table 1, for species that do react the effective ion molecule rate coefficient decreases with increasing cluster size. Not only does cluster size influence the effective ion molecule rate coefficient, it also establishes the ambient conditions under which the ion chemistry will be effective. As discussed in section 3.2, at high levels of water vapor small $(C_2H_5OH)_nH^+$ clusters are transformed into $(H_2O)_mH^+$ via

$$(C_2H_5OH)_nH^+ + mH_2O \rightarrow (H_2O)_mH^+ + nC_2H_5OH. \quad (8)$$

At high relative humidity a minimum cluster size is needed to preserve the $(C_2H_5OH)_nH^+$ ion chemistry and the selectivity of the technique. This means that the ethanol cluster ion size determines the selectivity and sensitivity for a given RH range. Consequently, the ethanol cluster ion size must be matched not only to the atmospheric species of interest but also to the ambient conditions.

[30] Of the species examined in this study the $(C_2H_5OH)_nH^+$ ion chemistry is best suited for the detection of DMSO. Since DMSO is one of the few species that reacts with large $(C_2H_5OH)_nH^+$ clusters, a high level of selectivity is inherent in this ion chemistry. The use of large ethanol clusters also reduces any sensitivity dependence on humidity seen in other CIMS techniques due to cluster ions with different numbers of water molecules reacting at different rates [*Seeley et al.*, 1997]. As demonstrated under ambient conditions during PEM-Tropics B, the combination of high selectivity, insensitivity to ambient RH levels, and

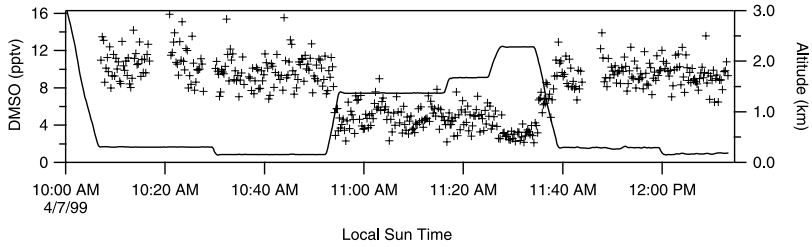

Figure 3. DMSO time series plot for midday boundary and buffer layer sampling during PEM-Tropics B flight 16. DMSO observations are represented by plus signs and the altitude by the solid line. Data are presented at a time resolution of 15 s.

fast time response and resolution makes this technique well suited for ambient measurements of DMSO.

[31] For many of the same reasons, this technique also shows considerable promise for the detection of NH_3. However, more attention needs to be paid to the $(C_2H_5OH)_nH^+$ cluster ion size than for detecting DMSO. With the largest $(C_2H_5OH)_nH^+$ clusters used in this study, NH_3 reaches an equilibrium that is dependent on temperature and ethanol concentrations. Consequently, the sensitivity could be strongly dependent on temperature and ethanol concentration of the reagent gas mixture. No other species in this study, except for DMSO, react with $(C_2H_5OH)_nH^+$ when using a 900 ppmv reagent gas mixture. Therefore, careful control of the $(C_2H_5OH)_nH^+$ cluster ion size distribution is critical to maintain the high selectivity while eliminating the difficulties of the equilibrium reaction. In addition, sampling and background issues need to be further addressed as highlighted by the presence of NH_3 related peaks shown in Figure 2b.

[32] Laboratory results also suggest that this method could be used to detect acetone and MVK under low ambient relative humidity conditions. Acetone is believed to be an upper tropospheric HO_x source and to partition reactive nitrogen into PAN [*Arnold et al.*, 1997; *Crawford et al.*, 1999; *Singh et al.*, 2000, 1995]. The low water levels in the upper troposphere may allow for fast-time resolution acetone measurements using small protonated ethanol clusters. The OH-initiated oxidation of isoprene has been found to yield MVK, methacrolein (MACR), and formeldehyde as major products [*Paulson et al.*, 1992; *Tuazon and Atkinson*, 1990]. Since MACR does not react with small $(C_2H_5OH)_nH^+$ clusters (see Table 2), this technique could potentially be used to differentiate between the isomers, MVK and MACR, when studying isoprene oxidation mechanisms. However, since isoprene oxidation is of most interest in the boundary layer, ambient relative humidity conditions are often too high for use of the small $(C_2H_5OH)_nH^+$ clusters. Further laboratory study examining the possibility of using the small $(C_2H_5OH)_nH^+$ cluster in conjunction of with a dryer to make boundary layer MVK measurements is needed.

5. Conclusions

[33] The reactivity of $(C_2H_5OH)_nH^+$ cluster ions has been found to be inversely related to cluster size, i.e., the larger clusters react with fewer species. Only two species, DMSO and NH_3, were found to react with the large $(C_2H_5OH)_nH^+$ cluster ions. DMSO reacts at or near the collisional rate with all size ethanol clusters examined. NH_3 also reacts with all size ethanol clusters, though it reaches an equilibrium with the larger clusters. For ambient measurements at RH > 50%, larger $(C_2H_5OH)_nH^+$ cluster ions must be utilized. Therefore, a high level of selectivity is inherent in the $(C_2H_5OH)_nH^+$ cluster ion chemistry. Interference testing shows that DMSO is not produced from DMS by ion processes in the ion-molecule reactor. $(C_2H_5OH)_nH^+$ cluster ion chemistry has been successfully used to measure DMSO from an aircraft platform during PEM-Tropics B. Laboratory studies suggest that this ion chemistry can be used to detect NH_3 under ambient atmospheric conditions.

[34] The ion-molecule reactor described here is viable for aircraft trace gas measurements. While the transport tube may limit the number of species that can be detected, due to the dissociation of weakly bound clusters, it eliminates possible interferences from those same clusters, makes the mass spectrum easier to interpret, and extends the sampling inlet outside the airplane's boundary layer.

[35] **Acknowledgments.** The author J.B. Nowak also acknowledges support from the NASA Earth System Science Fellowship program. The author F.L. Eisele would like to acknowledge partial support of this research by NASA grant NCC-1-301. The author D.D. Davis would like to acknowledge the partial support of this research by NASA grant NCC-1-306.

References

Arnold, F., V. Burger, B. DrosteFanke, F. Grimm, A. Krieger, J. Schneider, and T. Stilp, Acetone in the upper troposphere and lower stratosphere: Impact on trace gases and aerosols, *Geophys. Res. Lett.*, *24*(23), 3017–3020, 1997.

Arnold, S. T., J. V. Seeley, J. S. Williamson, P. L. Mundis, and A. A. Viggiano, New apparatus for the study of ion-molecule reactions at very high pressure (25–700 Torr): A turbulent ion flow tube (TIFT) study of the reaction of SF_6^- + SO_2, *J. Phys. Chem. A*, *104*(23), 5511–5516, 2000.

Arsene, C., I. Barnes, and K. H. Becker, FT–IR product study of the photo–oxidation of dimethyl sulfide: Temperature and O_2 partial pressure dependence, *Phys. Chem. Chem. Phys.*, *1*(24), 5463–5470, 1999.

Bandy, A., D. C. Thornton, B. W. Blomquist, S. Chen, T. P. Wade, J. C. Ianni, G. M. Mitchell, and W. Nadler, Chemistry of dimethyl sulfide in the equatorial Pacific atmosphere, *Geophys. Res. Lett.*, *23*(7), 741–744, 1996.

Barnes, I., V. Bastian, K. H. Becker, and D. Martin, Fourier–Transform Ir Studies of the Reactions of Dimethyl-Sulfoxide with OH, NO_3, and Cl Radicals, *ACS Symp. Ser.*, *393*, 476–488, 1989.

Barone, S. B., A. A. Turnipseed, and A. R. Ravishankara, Reaction of OH with dimethyl sulfide (DMS), 1, Equilibrium constant for OH + DMS reaction and the kinetics of the OH, DMS + O_2 reaction, *J. Phys. Chem.*, *100*(35), 14,694–14,702, 1996.

Bates, T. S., B. K. Lamb, A. Guenther, J. Dignon, and R. E. Stoiber, Sulfur emissions to the atmosphere from natural sources, *J. Atmos. Chem.*, *14*(1–4), 315–337, 1992.

Berresheim, H., D. J. Tanner, and F. L. Eisele, Real-time measurement of dimethyl-sulfoxide in ambient air, *Anal. Chem.*, *65*(1), 84–86, 1993.

Berresheim, H., P. H. Wine, and D. D. Davis, Sulfur in the atmosphere, in *Composition, Chemistry, and Climate of the Atmosphere*, edited by H. B. Singh, pp. 251–307, Van Nostrand Reinhold, New York, 1995.

Bohringer, H., D. W. Fahey, W. Lindinger, F. Howorka, F. C. Fehsenfeld, and D. L. Albritton, Mobilities of several mass-identified positive and negative-ions in air, *Int. J. Mass Spectrom. Ion Processes*, *81*, 45–65, 1987.

Charlson, R. J., J. E. Lovelock, M. O. reae, and S. G. Warren, Oceanic phytoplankton, atmospheric sulfur, cloud albedo and climate, *Nature*, *326*(6114), 655–661, 1987.

Chen, G., D. D. Davis, P. Kasibhatla, A. R. Bandy, D. C. Thornton, B. J. Huebert, A. D. Clarke, and B. W. Blomquist, A study of DMS oxidation in the tropics: Comparison of Christmas Island field observations of DMS, SO_2, and DMSO with model simulations, *J. Atmos. Chem.*, *37*(2), 137–160, 2000.

Coffman, D. J., and D. A. Hegg, A preliminary study of the effect of ammonia on particle nucleation in the marine boundary layer, *J. Geophys. Res.*, *100*(D4), 7147–7160, 1995.

Crawford, J., et al., Assessment of upper tropospheric HO_x sources over the tropical Pacific based on NASA GTE/PEM data: Net effect on HO_x and other photochemical parameters, *J. Geophys. Res.*, *104*(D13), 16,255–16,273, 1999.

Davis, D., G. Chen, P. Kasibhatla, A. Jefferson, D. Tanner, F. Eisele, D. Lenschow, W. Neff, and H. Berresheim, DMS oxidation in the Antarctic marine boundary layer: Comparison of model simulations and field observations of DMS, DMSO, $DMSO_2$, H_2SO_4(g), MSA(g), and MSA(p), *J. Geophys. Res.*, *103*(D1), 1657–1678, 1998.

De Bruyn, W. J., E. Swartz, J. H. Hu, J. A. Shorter, P. Davidovits, D. R. Worsnop, M. S. Zahniser, and C. E. Kolb, Henry's law solubilities and Setchenow coefficients for biogenic reduced sulfur species obtained from gas-liquid uptake measurements, *J. Geophys. Res.*, *100*(D4), 7245–7251, 1995.

Eisele, F. L., and D. R. Hanson, First measurement of prenucleation molecular clusters, *J. Phys. Chem. A*, *104*(4), 830–836, 2000.

Eisele, F. L., and D. J. Tanner, Ion-assisted tropospheric OH measurements, *J. Geophys. Res.*, *96*(D5), 9295–9308, 1991.

Eisele, F. L., and D. J. Tanner, Measurement of the gas-phase concentration of H_2SO_4 and methane sulfonic-acid and estimates of H_2SO_4 production and loss in the atmosphere, *J. Geophys. Res.*, *98*(D5), 9001–9010, 1993.

Feng, W. Y., and C. Lifshitz, The reactivity of neat and mixed proton-bound ethanol clusters, *Int. J. Mass Spectrom. Ion Processes*, *150*, 13–25, 1995.

Ferguson, E. E., Some aspects of negative ion chemistry, *Int. J. Mass Specrtom. Ion Processes*, *19*, 53–70, 1976.

Goldan, P. D., W. C. Kuster, and A. L. Albritton, A dynamic dilution system for the production of sub-ppb concentrations of reactive and labile species, *Atmos. Environ.*, *20*(6), 1203–1209, 1986.

Harvey, G. R., and R. F. Lang, Dimethylsulfoxide and dimethylsulfone in the marine atmosphere, *Geophys. Res. Lett.*, *13*(1), 49–51, 1986.

Huey, L. G., D. R. Hanson, and C. J. Howard, Reactions of SF_6^- and I^- with atmospheric trace gases, *J. Phys. Chem.*, *99*(14), 5001–5008, 1995.

Huey, L. G., E. J. Dunlea, E. R. Lovejoy, D. R. Hanson, R. B. Norton, F. C. Fehsenfeld, and C. J. Howard, Fast time response measurements of HNO3 in air with a chemical ionization mass spectrometer, *J. Geophys. Res.*, *103*(D3), 3355–3360, 1998.

Hunter, E. P., and S. G. Lias, Proton affinity evaluation, in NIST Chemistry WebBook, http://webbook.nist.gov, Natl. Inst. of Stand. and Technol., Galthersburg, Md., 2000.

Hynes, A. J., R. B. Stoker, A. J. Pounds, T. McKay, J. D. Bradshaw, J. M. Nicovich, and P. H. Wine, A mechanistic study of the reaction of OH with dimethyl-*d*6 sulfide: Direct observation of adduct formation and the kinetics of the adduct reaction with O_2, *J. Phys. Chem.*, *99*(46), 16,967–16,975, 1995.

Kilpatrick, F. W., An experimental mass-mobility relation for ions at atmospheric pressure, paper presented at 19th Annual Conference on Mass Spectroscopy, Am. Soc for Mass Spectrom., Atlanta, Ga., 1971.

Kim, S. H., and G. E. Spangler, Ion mobility spectrometry/mass spectrometry (IMS/MS) of two structurally different ions having identical ion mass, *Anal. Chem.*, *57*(2), 567–569, 1985.

Lakdawala, V. K., and J. L. Moruzzi, Measurements of attachment coefficients and ionic mobilities in SF_6-nitrogen mixtures over the low-energy range 1.2–4.0 eV, *J. Phys. D*, *13*, 1439–1445, 1980.

Lovejoy, E. R., Ion trap studies of H^+ $(H_2SO_4$)(m)(H_2O)(n) reactions with water, ammonia, and a variety of organic compounds, *Int. J. Mass Spectrom.*, *191*, 231–241, 1999.

Makela, J. M., V. Jokinen, T. Mattila, A. Ukkonen, and J. Keskinen, Mobility distribution of acetone cluster ions, *J. Aerosol. Sci.*, *27*(2), 175–190, 1996.

Mauldin, R. L., D. J. Tanner, and F. L. Eisele, A new chemical ionization mass spectrometer technique for the fast measurement of gas phase nitric acid in the atmosphere, *J. Geophys. Res.*, *103*(D3), 3361–3367, 1998.

Mauldin, R. L., et al., Measurements of OH aboard the NASA P-3 during PEM-Tropics B, *J. Geophys. Res.*, *106*(D23), 32,657–32,666, 2001.

Nowak, J. B., et al., Airborne observations of DMSO, DMS, and OH at marine tropical latitudes, *Geophys. Res. Lett.*, *28*(11), 2201–2204, 2001.

Paulson, S. E., R. C. Flagan, and J. H. Seinfeld, Atmospheric photooxidation of isoprene, 1, The hydroxyl radical and ground-state atomic oxygen reactions, *Int. J. Chem. Kinet.*, *24*(1), 79–101, 1992.

Sciare, J., and N. Mihalopoulos, A new technique for sampling and analysis of atmospheric dimethylsulfoxide (DMSO), *Atmos. Environ.*, *34*(1), 151–156, 2000.

Seeley, J. V., R. A. Morris, and A. A. Viggiano, Rate constants for the reactions of CO_3-(H_2O)(n = 0–5) + SO_2: Implications for CIMS detection of SO_2, *Geophys. Res. Lett.*, *24*(11), 1379–1382, 1997.

Singh, H. B., M. Kanakidou, P. J. Crutzen, and D. J. Jacob, High-concentrations and photochemical fate of oxygenated hydrocarbons in the global troposphere, *Nature*, *378*(6552), 50–54, 1995.

Singh, H., et al., Distribution and fate of selected oxygenated organic species in the troposphere and lower stratosphere over the Atlantic, *J. Geophys. Res.*, *105*(D3), 3795–3805, 2000.

Sorensen, S., H. FalbeHansen, M. Mangoni, J. Hjorth, and N. R. Jensen, Observation of DMSO and CH_3S(O)OH from the gas phase reaction between DMS and OH, *J. Atmos. Chem.*, *24*(3), 299–315, 1996.

Streit, G. E., Negative ion chemistry and electron affinity of SF_6, *J. Chem. Phys.*, *77*, 826–833, 1982.

Su, T., and W. J. Chesnavich, Parameterization of the ion-polar molecule collision rate constant by trajectory calculations, *J. Chem. Phys.*, *76*, 5183–5185, 1982.

Tammet, H., Size and mobility of nanometer particles, clusters and ions, *J. Aerosol. Sci.*, *26*(3), 459–475, 1995.

Tuazon, E. C., and R. Atkinson, A product study of the gas-phase reaction of isoprene with the OH radical in the presence of NO_x, *Int. J. Chem. Kinet.*, *22*(12), 1221–1236, 1990.

Turnipseed, A. A., S. B. Barone, and A. R. Ravishankara, Reaction of OH with dimethyl sulfide, 2, Products and mechanisms, *J. Phys. Chem.*, *100*(35), 14,703–14,713, 1996.

Urbanski, S. P., R. E. Stickel, and P. H. Wine, Mechanistic and kinetic study of the gas-phase reaction of hydroxyl radical with dimethyl sulfoxide, *J. Phys. Chem. A*, *102*(51), 10,522–10,529, 1998.

Viggiano, A. A., In-situ mass-spectrometry and ion chemistry in the stratosphere and troposphere, *Mass Spectrom. Rev.*, *12*(2), 115–137, 1993.

Weber, R. J., P. H. McMurry, L. Mauldin, D. J. Tanner, F. L. Eisele, F. J. Brechtel, S. M. Kreidenweis, G. L. Kok, R. D. Schillawski, and D. Baumgardner, A study of new particle formation and growth involving biogenic and trace gas species measured during ACE 1, *J. Geophys. Res.*, *103*(D13), 16,385–16,396, 1998.

Williams, E. J., et al., An intercomparison of five ammonia measurement techniques, *J. Geophys. Res.*, *97*(D11), 11,591–11,611, 1992.

Yin, F. D., D. Grosjean, R. C. Flagan, and J. H. Seinfeld, Photooxidation of dimethyl sulfide and dimethyl disulfide, 2, Mechanism evaluation, *J. Atmos. Chem.*, *11*(4), 365–399, 1990a.

Yin, F. D., D. Grosjean, and J. H. Seinfeld, Photooxidation of dimethyl sulfide and dimethyl disulfide, 1, Mechanism development, *J. Atmos. Chem.*, *11*(4), 309–364, 1990b.

C. Cantrell, F. L. Eisele, E. Kosciuch, and R. L. Mauldin III, Atmospheric Chemistry Division, National Center for Atmospheric Research, P.O. Box 3000, Boulder, CO 80305-3000, USA. (cantrell@ucar.edu; eisele@ucar.edu; kosciuch@ucar.edu; mauldin@ucar.edu)

D. Davis, G. Huey, and D. Tanner, School of Earth and Atmospheric Sciences, Georgia Institute of Technology, 221 Bobby Dodd Way, Atlanta, GA 30332, USA. (douglas.davis@eas.gatech.edu; greg.huey@eas.gatech.edu; tanner@eas.gatech.edu)

J. Nowak, Aeronomy Laboratory, NOAA, 325 Broadway, R/AL-7, Boulder, CO 80305, USA. (jnowak@al.noaa.gov)